Preparation of fluorescence-encoded microspheres in a core–shell structure for suspension arrays

Zhiling Zhang, Yao Long, Jianbo Pan and Xiaomei Yan*

Fluorescence-encoded microspheres are widely used in the detection and analysis of biological molecules, especially in suspension arrays. Here, we report an efficient strategy for the preparation of fluorescence-encoded polystyrene microspheres with desirable optical and surface properties. The micron-sized, monodisperse polystyrene seed beads were first synthesized by dispersion polymerization. Then, dye molecules and carboxyl functional groups were copolymerized on the surface of the seed beads by forming a core–shell structure. Rhodamine 6G (R6G) was used as a model dye molecule to prepare the fluorescent beads, and the fluorescence intensity of the beads can be precisely controlled by adjusting the quantity of R6G. These fluorescent beads were characterized by environmental scanning electron microscopy, laser scanning confocal microscopy, and spectrofluorometry. The differences of the fluorescence spectra between fluorescent beads and R6G in solution were investigated. Twelve kinds of fluorescent beads encoded with different R6G fluorescence intensities were prepared, and they can be clearly distinguished on a conventional flow cytometer. Furthermore, the encoded beads are stable in water and resistant to photobleaching, which is crucial for their potential applications in diagnostic assays and imaging. Detection of human alpha fetoprotein antigen *via* a sandwich microsphere-based immunoassay yielded a detection limit of 80 pg mL^{-1}, demonstrating that the fluorescence-encoded microspheres synthesized herein are efficient in serving as the microcarriers in suspension arrays. As both the encoding and functionalizing procedures are made simultaneously, the newly designed technique is extremely simple and time-saving. Moreover, it could be readily applicable to the preparation of a wide size range of fluorescent particles made by polymerization.

Introduction

Suspension arrays have attracted increasing interest recently due to their promising applications in medical diagnosis, protein detection, genetic and genomic analysis, drug screening, and other fields.[1–5] Compared to enzyme-linked immunosorbent assays (ELISAs), suspension arrays provide multiplexed analysis, faster binding kinetics, and equal or higher detection sensitivity.[6] As an evolution of the planar array, suspension array technology offers advantages like higher flexibility in array preparation, reduced cost, greater reliability, and superior detection sensitivity.[7–9] In suspension arrays, micron-sized microspheres (so-called beads) typically are used as the microcarriers, and multiple target analytes can be detected simultaneously by mixing the different microcarriers (attached with corresponding capture probes) in the same vial. The code on each microcarrier allows the ligand bound (or compound attached) to the surface of the microspheres to be identified.[10] For example, the Luminex Corporation (Austin, TX, USA) has developed a multiplexed microsphere-based system that enables the assay of up to 100 different probes in one sample tube or well.[11,12]

One of the biggest challenges for suspension arrays is to prepare encoded microspheres with large encoding capacity and good functionality in a simple and reproducible way. Many encoding strategies have been proposed for beads that are used in drug screening and diagnostic applications, including physical, graphical, electronic, and spectrometric encoding methods.[9,10] Physical characteristics of the beads, such as size[13] and diffractive index,[14] are usually used in bead encoding, but this approach is quite limited in the number of beads that can be uniquely encoded. Graphical encoding by spatial modulation of a material or its properties provides an alternative way to fabricate encoded beads,[15] but the decoding process is slow, expensive, and not amenable to automation. Radio-frequency (rf) tags have been proposed for labeling reaction vessels[16,17] and individual microcarriers.[18] Although the size of rf devices is relatively large compared with typical microcarriers (1–50 μm), the technique is promising because of the virtually unlimited number of unique codes.[10] Spectrometric encoding methods have been developed that take advantage of chemical tags with a variety of spectroscopic entities, such as fluorescent molecules, molecules with specific vibrational or nuclear magnetic resonance signatures, quantum dots (QDs), and photonic crystals that provide coded elements.[10,19–22] Among all of the optical encoding methods, fluorescence-encoded technology is the most popular approach because of its simple encoding process, large encoding capacity, cost effectiveness, and rapid signal acquisition using conventional flow cytometry.[23–25]

Department of Chemical Biology, College of Chemistry and Chemical Engineering, The Key Laboratory for Chemical Biology of Fujian Province, Key Laboratory of Analytical Science, Xiamen University, Xiamen, 361005, China. E-mail: xmyan@xmu.edu.cn; Fax: +86-592-2189959; Tel: +86-592-2184519

This journal is © The Royal Society of Chemistry 2010

J. Mater. Chem., 2010, **20**, 1179–1185 | 1179

Organic fluorophores and semiconductor quantum dots are the two most important elements employed for fluorescence-based bead encoding. Quantum dots have wide excitation and narrow emission spectra, and are brighter and more photostable than fluorescent dye molecules; these properties make them attractive for bead encoding.[26] However, QDs are difficult to synthesize and are expensive. Up to now, most of the suspension arrays reported in the literature use organic dye-encoded beads as the microcarriers; these beads can be prepared by copolymerization of reactive dyes, covalent attachment of dyes to beads, adsorption, or solvent swelling.[27–33] Copolymerization of reactive dyes avoids fluorescence leakage of the product fluorescent beads, but the synthesis of the dye-linked monomer is required.[31] Covalent attachment of dyes to beads is also a good method for obtaining fluorescent beads without dye leaching.[27,29] The adsorption method (*e.g.*, the layer-by-layer technique) is a simple and cost-effective approach for fabricating fluorescent beads.[28,30,33] The solvent swelling method is produced by swelling the beads with organic solvent, which allows the dye molecules to transport into the beads.[32] Using this latter strategy, Luminex Corp (Austin, TX) succeeded in preparing their xMAP arrays. Although solvent swelling method is effective, the encoding steps are laborious and time-consuming.

Besides optical coding of the beads, surface modification with functional groups is also vital to the fabrication of beads. The number of functional groups is critical for ensuring that a sufficient number of capture probes can be immobilized on the surface of the bead. A wide range of active chemical groups are now available for covalent coupling of biomolecules onto the surface of the bead, including carboxyl, amine, aldehyde, hydroxyl, thiol, epoxy groups, *etc.*[22,34–36] Among them, carboxyl groups and amines are the two most popular functional groups used for bead surface modification because they can be easily attached to biomolecules *via* well-established carbodiimide or glutaraldehyde chemistry.

In the present paper, we report a facile and effective method for fabricating fluorescence-encoded polystyrene microspheres with carboxyl functionalities on the surface. Rhodamine 6G (R6G) was used as a model dye molecule to prepare the fluorescent beads because it is biocompatible, highly fluorescent, cost effective, and hydrophobic. The fluorescence intensities of the beads can be precisely controlled by adjusting the quantity of R6G added. The stability of the beads upon longtime storage was investigated. The feasibility of using the synthesized fluorescence-encoded beads in clinical applications was demonstrated with human alpha fetoprotein (AFP) antigen detection *via* a sandwich microsphere-based immunoassay.

Experimental section

Materials

Divinyl benzene (DVB, 80%) was obtained from Fluka. Rhodamine 6G (R6G) was purchased from Acros Organics (Geel, Belgium). Styrene was obtained from Xilong Chemical Co., Ltd. (Guangdong, China) and was washed with 1.25 M sodium hydroxide solution to remove potential inhibitors. Analytical grade potassium persulfate (KPS), azodiisobutyronitrile (AIBN), polyvinylpyrrolidone (PVP K-30, $M_w = 40\,000$ g mol^{-1}), ethanol

(99.5%), methacrylic acid (MAA, 98%), and dodecyl sulfonic acid sodium (SDS) were purchased from Sinopharm Chemical Reagent Co., Ltd. (Shanghai, China). AIBN was purified by recrystallization from ethanol. 1-Ethyl-3-(3-dimethylaminopropyl)carbodiimide hydrochloride (EDC), sulfo-*N*-hydroxy-succinimide (Sulfo-NHS), and Sulfo-NHS-biotin were obtained from Pierce (Illinois, USA). The AFP antigen and its monoclonal antibodies were obtained from Boson Biotechnology Corp. (Xiamen, China). AFP reporter monoclonal antibody was biotinylated according to the manufacture's instructions (Pierce). Highly fluorescent protein allophycocyanin (APC) conjugated streptavidin was purchased from Molecular Probes (Oregon, USA). All other chemicals were obtained from Sigma. Deionized water was used in all experiments.

Preparation of polystyrene seed beads by dispersion polymerization.[37]

Polystyrene seed beads were prepared by dispersion polymerization in a 100 mL three-necked round-bottom glass reactor equipped with a nitrogen inlet, a thermometer and a mechanical rabble. PVP K-30 (0.375 g) dissolved in 50 mL of ethanol was placed into the reactor. After nitrogen purging, the reactor was immersed in an oil bath equipped with a thermostat set at $70 \pm 0.5\,^\circ$C for 5 min. Then, AIBN (0.125 g) dissolved in a mixture of styrene (14.5 g) and MAA (0.127 g) was added to the reactor. The polymerization was conducted for 24 h at a stirring rate of 180 rpm. After cooling down to room temperature, the resulting beads were washed by centrifugation/redispersion cycles with ethanol and DI water three times each to remove by-products. Finally, the beads were dried in a vacuum oven for 24 h.

Preparation of functional fluorescent beads in a core-shell structure

The polystyrene seed beads were first diluted to 20% solid content with DI water, and 5 mg mL^{-1} SDS was added to equal volume of the 20% polystyrene beads; the resulting mixture was stirred gently in a microcentrifuge tube for 15 min. Unless otherwise stated, 500 μL of the dispersed polystyrene beads as seeds and 12.5 mg of KPS as initiator were placed into a 10 mL one-necked round-bottom glass reactor. Then 25 μL of undecylenic acid/methanol (1 : 10, v/v) and 10 μL of DVB/methanol (1 : 100, v/v) solution were added to the reactor. Fluorescent dye (32 μL of 1 mg mL^{-1} R6G in a water solution) was added into the dispersion. After then, 2 mL of DI water was added to the reactor and the suspension was stirred at 600 rpm for 5 min. After deoxygenation, the suspension was stirred at 320 rpm with a magnetic stirrer and the polymerization was allowed to proceed at $70 \pm 0.5\,^\circ$C for 7.5 h. The beads were then centrifuged and rinsed with ethanol and DI water three times each to remove excess reagents. Finally, the beads were dispersed with 2 mL of water and stored at 4 °C.

Microscopic characterization of beads

The microstructures of the seed beads and the fluorescent beads were characterized using scanning electron microscopy (SEM, XL-30, Philips Corp.) at an acceleration voltage of 20 kV. In order to measure the average bead diameter and the

coefficient of variation of the beads, 200 individual beads in the scanning electron micrographs were counted for each specimen. The shell thickness (ST) was calculated as follows: $ST = (d_2 - d_1)/2$, where d_1, d_2 denote the average diameter of the seed beads and fluorescent beads, respectively. For confocal fluorescence microscope measurements, the fluorescent beads were deposited onto a clean glass slide and dried under an infrared lamp. Fluorescence micrographs were captured with a confocal laser scanning microscope (TCS SP5, Leica) with the excitation wavelength set at 488 nm and emission wavelength set at 530–700 nm, using a 100× oil immersion objective lens (NA of 1.2).

Fluorescence spectroscopy measurement

The fluorescence spectra of fluorescent beads and of R6G in solution were taken on a Hitachi F-4500 fluorometer with both the emission and excitation slit widths set at 5 nm. The fluorescence emission spectra were recorded using an excitation wavelength (λ_{ex}) of 488 nm, and the fluorescence excitation spectra were recorded using an emission wavelength (λ_{em}) of 560 nm. Before the measurement, the bead suspension was diluted 100-fold to 5.0×10^{-4} mg mL^{-1}, and the R6G solution was prepared at a concentration of 1.0×10^{-4} mg mL^{-1}.

Flow cytometric analysis of fluorescent beads

Flow cytometric analysis was performed on a FACSAria flow cytometer (BD Biosciences, San Jose, CA, USA) with a 488 nm excitation laser. The microspheres were gated on forward light scatter and side (90°) light scatter. The R6G fluorescence signal was measured on the FL2 channel (PE channel, 575/26 nm band pass filter for detecting light signals from 562 to 588 nm) for the decoding of the fluorescence-encoded beads. Median fluorescence intensity was reported by analyzing 10 000 gated beads for each bead set by BD FACSDiVa™ Software.

Covalent coupling of monoclonal antibodies to microspheres

A two-step coupling procedure was used to covalently attach the AFP capture MAb to the R6G-doped fluorescent beads *via* amide bond formation between the carboxyl groups on the bead surface and the primary amine groups of the protein. Briefly, 5×10^6 of the lab-prepared R6G encoded beads were pipetted into 80 μL of activation buffer (10 mM sodium acetate, pH 5.4), to which freshly made solutions of NHS (10 μL, 50 mg mL^{-1}) and EDC (33 μL, 100 mg mL^{-1}) in the activation buffer were added. After vortexing (30 s) and incubation at room temperature (20 min), excess EDC/NHS was removed by centrifugation/resuspension. After washing twice with 500 μL activation buffer, the microspheres were resuspended in 500 μL of the coupling buffer (same composition as the activation buffer), to which AFP capture MAb solution (10 μL, 2 mg mL^{-1}) was added. After incubating the microsphere and MAb mixture on a shaker at room temperature for 3.5 h, the MAb-bearing microspheres were washed twice with 500 μL washing buffer (PBS/0.05% Tween 20) and then stored in 500 μL blocking/storage buffer (PBS/1% BSA/ 0.05% sodium azide) at 4 °C.
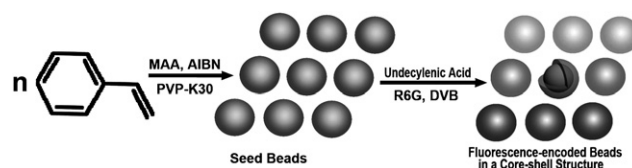
Procedure for microsphere-based immunoassay

Fifty thousand MAb-coupled beads were added to 50 μL of AFP dilution prepared in the incubation buffer (PBS/1% BSA/0.2% Tween 20). Following incubation at 37 °C for 45 min, two washes were carried out to remove the unbound analytes. Then the self-prepared biotinylated AFP reporter MAb (50 μL, 10 μg mL^{-1}) was added, and the mixture was incubated at 37 °C for 30 min. After two washes with 500 μL washing buffer, APC-conjugated streptavidin (50 μL, 10 μg mL^{-1}) was added. Following a 20 min incubation at 37 °C, the beads were washed twice with washing buffer. In the end, the beads were resuspended in 300 μL of PBS for analysis on the FACSAria flow cytometer using a 633 nm excitation laser and the FL 4 (660/20 nm band pass filter for detecting light signals from 650 to 670 nm) channel for the APC fluorescence detection.

Results and discussion

Synthesis and morphological characterization of seed beads and fluorescent beads

To generate functional fluorescent microspheres, we attempted to coat the polystyrene seed beads with fluorescent dye and carboxyl groups simultaneously. During the copolymerization process, undecylenic acid, DVB, R6G, and potassium persulfate were added into the suspension of seed beads as the functional monomer, cross-linking reagent, dye molecule, and initiator, respectively. (Scheme 1). In order to characterize the morphology of the seed beads and to investigate the effect of carboxylation and fluorescence encoding on the size distribution of the fluorescent beads, SEM images of the seed beads and the fluorescence-encoded beads were taken and compared. As shown in Fig. 1a, the seed beads prepared by dispersion polymerization were spherically shaped and monodisperse. The average diameter was 3.77 μm with a size distribution coefficient of variation (CV) of 2.4%. Compared to the seed beads, the fluorescent beads (Fig. 1b) were also perfectly spherical with a slightly larger average diameter of 3.82 μm. Meanwhile, the size distribution was narrower, and the CV decreased slightly to 1.7%. Clearly, the carboxylation and fluorescence-encoding process did not alter the monodispersity of the seed beads. The thickness of the fluorescence shell was calculated to be 25 nm. The thinness of this layer could be attributed to the small amount of DVB and undecylenic acid monomers added, and to the short swelling time.[38,39] Note that the thickness of the shell is negligible compared to the bead diameter, thus the size of the fluorescent beads can be closely controlled during the synthesis of polystyrene seed beads.

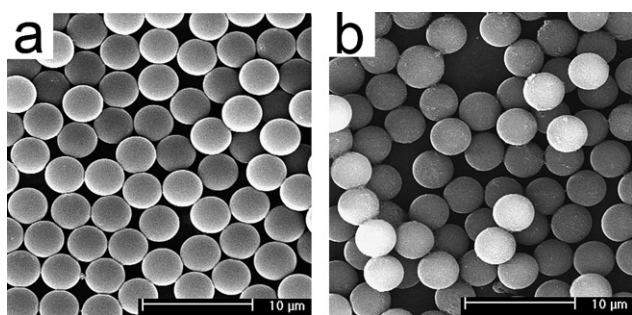**Scheme 1** The protocol for the preparation of fluorescence-encoded microspheres.

This journal is © The Royal Society of Chemistry 2010

J. Mater. Chem., 2010, **20**, 1179–1185 | 1181

Fig. 1 The SEM images of the seed beads (a) and the fluorescent beads (b).

Effects of undecylenic acid and DVB amounts on the fluorescence-encoding of the seed beads

The influence of the undecylenic acid and DVB quantities on the size distribution and fluorescence intensity of the R6G encoded fluorescent beads was examined. SEM images shown in Fig. 2a–d indicate that when the undecylenic acid amount was small, the fluorescent beads were uniformly distributed in spheres. When the undecylenic acid/methanol quantity was increased to 48 µL, particle adhesion can be observed (Fig. 2c). Upon further increasing the amount of undecylenic acid/methanol to 64 µL, the beads became inhomogeneous as shown in Fig. 2d. Fig. 3a shows the relationship between the undecylenic acid quantity and the fluorescence intensity of the fluorescent beads as measured by flow cytometry. Because non-uniform beads may clog the flow cell of the flow cytometer (and, in addition, these beads would not be suitable for applications in suspension arrays), fluorescent beads prepared with undecylenic acid/methanol quantities larger than 32 µL were not measured. As displayed in Fig. 3a, within the

undecylenic acid amount range that was examined, the fluorescent intensity of the beads increased concurrently with the increasing amounts of undecylenic acid. This can be attributed to the easier swelling of polystyrene seed beads and, consequently, the easier penetration of dye molecules in the presence of more undecylenic acid. Similar effects on the size distribution of the fluorescent beads were observed for DVB. When the DVB/methanol amount was increased to 448 µL (Fig. 2h), the size distribution of the fluorescent beads deteriorated severely (note that the scale bar of Fig. 2 h is different from the others). On the other hand, the fluorescence intensity of the beads went up with increasing DVB amounts when the DVB quantity was low (Fig. 3b). This could be attributed to greater amounts of shell cross-linking in the presence of more DVB, leading to more R6G trapped in the shell. However, with the further increase in DVB
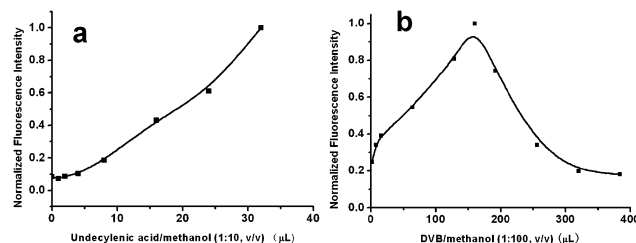

Fig. 3 (a) Relationship between the amount of undecylenic acid and the fluorescence intensity of the fluorescent beads measured by flow cytometry. Samples were prepared from 0.05 g of seed beads, 12.5 mg of KPS, 1.25 mg of SDS, 10 µL of DVB/methanol (1 : 100, v/v) solution, 32 µg of R6G, and 2 mL of water. (b) Relationship between the DVB amount and the fluorescence intensity of the fluorescent beads measured by flow cytometry. Samples were prepared from 0.05 g of seed beads, 12.5 mg of KPS, 1.25 mg of SDS, 25 µL of undecylenic acid/methanol (1 : 10, v/v), 32 µg of R6G, and 2 mL of water.
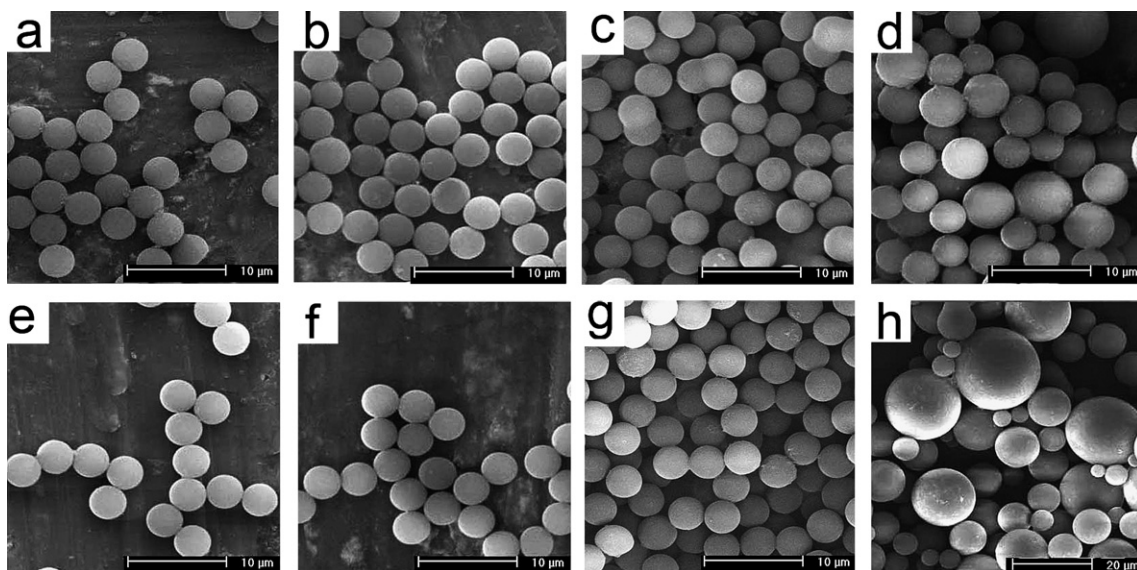

Fig. 2 SEM images of the fluorescent polystyrene beads prepared with different combinations of undecylenic acid and DVB amount. Samples a to d were prepared from 0.05 g of seed beads, 12.5 mg of KPS, 1.25 mg of SDS, 10 µL of DVB/methanol (1 : 100, v/v), 32 µg of R6G, and 2 mL of water. The amounts of undecylenic acid/methanol (1 : 10, v/v) were 4 µL (a), 16 µL (b), 48 µL (c), and 64 µL (d). Samples e to h were prepared from 0.05 g of seed beads, 12.5 mg of KPS, 1.25 mg of SDS, 25 µL of undecylenic acid/methanol (1 : 10, v/v), 32 µg of R6G, and 2 mL of water. The amounts of DVB/methanol (1 : 100, v/v) were 32 µL (e), 128 µL (f), 192 µL (g), and 448 µL (h).

quantity, too many dye molecules were incorporated into the shell, and fluorescence quenching occurred.

Confocal fluorescence microcopy images and spectral properties of fluorescent beads

Confocal fluorescence microscopy is often used to examine the distribution of dye in the beads. Herein, the confocal fluorescence microscopic graph of the beads illustrates the ring structure of the fluorescent beads, confirming that R6G was uniformly located on the bead surface without significant penetration (Fig. 4a). Combined with the effects of undecylenic acid and DVB on the fluorescent beads, the mechanism of R6G doping may be explained as follows: first, undecylenic acid swelled the polystyrene beads,[39,40] then R6G penetrated the bead surface based on the principle of "like dissolves like" to lower the free energy of the system.[41] With the cross-linking polymerization of DVB and undecylenic acid, R6G was trapped on the shell of the beads. In order to illustrate this mechanism, rhodamine B was also used to encode the beads. A 7% fluorescence leakage into water was observed upon overnight storage, in contrast, no fluorescence leakage was found for R6G encoded beads. This difference could be attributed to the stronger hydrophobic nature of R6G as compared to rhodamine B. Fluorescence measurements were carried out to compare the spectral properties of R6G in aqueous solution and doped within fluorescent beads (Fig. 4b). It is clear that while the fluorescence emission peaks of R6G in fluorescent beads and in water were the same at 560 nm, the excitation peak of R6G incorporated into the beads produced an 8 nm red shift. This shift is probably ascribed to the aggregation of R6G in the shell.[41,42] To detect the fluorescence dispersity of the fluorescent beads, the fluorescent beads were detected on a conventional flow cytometer. Flow cytometric analysis of 10 000 fluorescent beads showed that the standard deviation of the fluorescence intensity of the beads was approximately 6%. This value is close to that of the seed beads (5.6% variation based on FACS), suggesting that the observed fluorescence signal variation is mainly a function of the size uniformity of the seed beads.

Fluorescence encoding of microspheres in a core–shell structure

In order to prepare fluorescence beads with different codes, the effect of R6G quantity on the fluorescence intensity of the beads was studied by flow cytometry. As shown in Fig. 5, when the
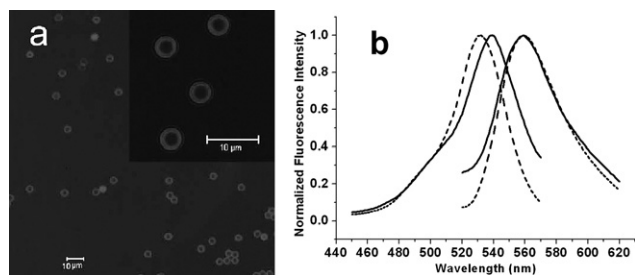
Fig. 4 (a) Confocal micrograph of fluorescent polystyrene beads. (b) Fluorescence excitation and emission spectra of R6G in water (dashed line) and R6G encoded fluorescent beads dispersed in water (solid line).
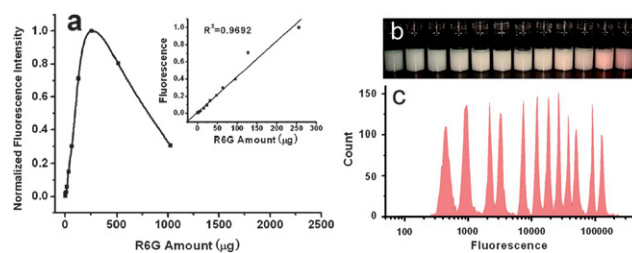
Fig. 5 (a) Relationship between the R6G amount and the fluorescence intensity of the fluorescent beads measured by flow cytometry. Correlation of the fluorescence intensity and the R6G quantity is given in the inset. (b) True picture of R6G-encoded beads prepared from 0.05 g of seed beads, 12.5 mg of KPS, 1.25 mg of SDS, 25 μL of undecylenic acid/methanol (1 : 10, v/v), 10 μL of DVB/methanol (1 : 100, v/v), and 2 mL of water. From left to right, the quantity of R6G was of 1, 2, 4, 8, 16, 24, 32, 48, 64, 96, 128, and 256 μg, respectively. (c) Flow cytometric analysis of the bead array mixture.

R6G amount was less than 256 μg, the fluorescence intensity of the beads increased linearly with the R6G quantity (inset of Fig. 5a). As a result, it is easy to predict and fabricate beads with precise fluorescence control by adjusting the amount of dye added. However, a further increase of dye quantity may lead to an unfavorable decrease of the bead fluorescence due to self-quenching (Fig. 5a). Therefore, it is important to choose the proper amount of dye for encoding beads. Fluorescent beads prepared with 1, 2, 4, 8, 16, 24, 32, 48, 64, 96, 128, and 256 μg of R6G are shown in Fig. 5b. Obviously, the bead color becomes deeper with increasing amounts of R6G. These beads were mixed to form a bead array, and their fluorescence was measured on a flow cytometer. As shown in Fig. 5c, the different fluorescence intensities of the beads can be easily decoded on the FL2 channel of the flow cytometer, and twelve kinds of fluorescent beads encoded with different R6G quantities can be distinguished completely without obvious overlap. This experiment demonstrated that we can obtain fluorescence-encoded beads through the precise control of the dye quantity during the carboxylation and fluorescence-encoding process.

Stability of the fluorescence-encoded beads

For the longtime storage of fluorescent beads, the stability of the functional fluorescence encoded beads was investigated by measuring the fluorescence intensity of the beads on a flow cytometer every four months upon storage in water at 4 °C. The same reference bead sample was measured in parallel every time. It was found that there was no fluorescence dye leakage for the fluorescent beads over eight months of storage time (data not shown). Therefore fluorescent beads prepared by our approach can be stored for a relatively long time which is important for their potential applications in suspension array detection. The photobleaching behavior of the R6G dye molecules incorporated into the polystyrene beads was studied on a spectrofluorometer. The fluorescent beads were placed in a 1 cm light path cuvette and were exposed to xenon lamp excitation on a Hitachi F-4500 fluorometer for 1 h and the stability of the fluorescence emission was monitored. The excitation and emission wavelengths were set at 488 nm and 565 nm, respectively. The R6G dye dissolved in
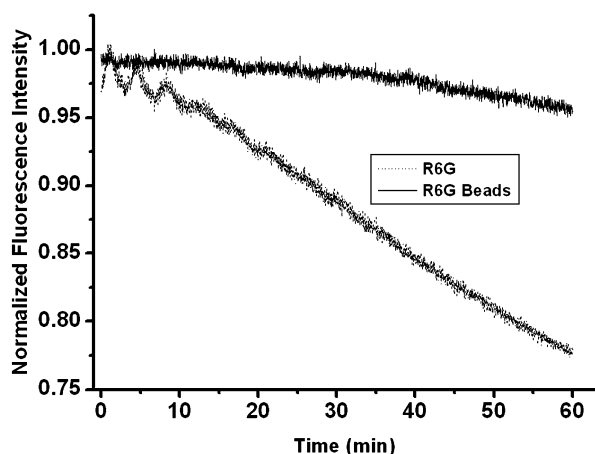
Fig. 6 Photobleaching behavior of fluorescent beads (solid line) and free dye (dashed line).

water was compared in parallel. Fig. 6 indicates that for R6G dye molecules dissolved in water, a gradual decrease in the fluorescence intensity was observed with increased exposure time. Upon 1 h of exposure, the fluorescence intensity decreased about 25%. In contrast, the fluorescence intensity of R6G doped in the polystyrene beads showed an insignificant decrease with the exposure duration. This result can be attributed to a decrease in the non-radiative decay rates for the dyes upon encapsulation in the beads.[43,44] Therefore, the fluorescent beads were more photostable when incorporated into the shell.

Application in immuno-detection

The applicability of these fluorescent beads in suspension array detection was examined in a microsphere-based sandwich immunoassay for AFP detection. As illustrated schematically in Fig. 7a, mouse-*anti*-human AFP monoclonal antibody was covalently coupled to the beads. These beads were used to capture AFP in solution. Biotinylated AFP reporter monoclonal antibody and streptavidin-APC were used to label the analytes captured on the beads, and the APC fluorescence was detected on the FL4 channel of the flow cytometer. Fig. 7b shows the relationship between the AFP concentration and the fluorescence intensity of the beads. When the AFP concentration was below 25 ng mL^{-1}, the fluorescence intensity increased with increases in AFP concentration, but then the fluorescence reached a plateau. The calculated detection limit of AFP was 80 pg mL^{-1}, based on the 3-fold standard deviation of the blank sample. This detection sensitivity is sufficient for AFP detection in clinical diagnosis.
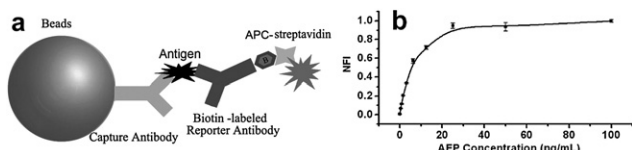

Fig. 7 (a) A schematic diagram of a flow cytometric microsphere-based immunoassay for AFP antigen detection. (b) The relationship between AFP concentration and the fluorescence intensity of APC-tagged reporter antibody bound to the bead surface. Error bars represent standard deviations, and NFI represents normalized fluorescence intensity.

Conclusions

In summary, we have developed a simple method to prepare fluorescence-encoded microspheres with desirable optical and surface properties. The micron-sized, monodisperse polystyrene seed beads were first synthesized by dispersion polymerization. Next, dye molecules and carboxyl functional groups were copolymerized on the surface of the seed beads by forming a core–shell structure. SEM images showed that there were no remarkable changes in either size or shape between the seed beads and the fluorescent bead. So, the size of the fluorescent beads can be closely controlled during the synthesis of polystyrene seed beads. Confocal microscope images illustrated that the bead is composed of fluorescent dye layer around core particle. R6G was incorporated into the shell *via* hydrophobic interactions, and the fluorescence intensity of the beads can be precisely controlled by adjusting the dye quantity. Twelve different sets of fluorescent beads were obtained and their fluorescence intensities can be distinguished on a flow cytometer. These fluorescent beads have been demonstrated to be photostable and resistant to photobleaching. Immunoassay performance for AFP detection indicated that the fluorescent beads facilitate efficient attachment of bio-probes and therefore enable high detection sensitivity. These fluorescent beads hold much promise for multiplexing in the future by using beads conjugated with different capture probes for different targets. Though R6G was used in the present work as a model dye molecule for fluorescence-encoding of the beads, the proposed method should be applicable to a wide variety of hydrophobic materials and polymer colloids. In addition, both the encoding and functionalization procedure are performed simultaneously, which is extremely simple and time-saving. Moreover, this newly proposed encoding strategy could be readily applicable to the preparation of a wide size range of fluorescent particles made by polymerization.

Acknowledgements

References

1 S. Brenner, M. Johnson, J. Bridgham, G. Golda, D. H. Lloyd, D. Johnson, S. Luo, S. McCurdy, M. Foy, M. Ewan, R. Roth, D. George, S. Eletr, G. Albrecht, E. Vermaas, S. R. Williams, K. Moon, T. Burcham, M. Pallas, R. B. DuBridge, J. Kirchner, K. Fearon, J. Mao and K. Corcoran, *Nat. Biotechnol.*, 2000, **18**, 630.
2 M. Trau and B. J. Battersby, *Adv. Mater.*, 2001, **13**, 975.
3 J. P. Nolan and F. F. Mandy, *Cell Mol. Biol. (Noisy-le-grand)*, 2001, **47**, 1241.
4 I. V. Jani, G. Janossy, D. W. Brown and F. Mandy, *Lancet Infect. Dis.*, 2002, **2**, 243.
5 L. A. Ugozzoli, *Clin. Chem.*, 2004, **50**, 1963.
6 M. F. Elshal and J. P. McCoy, *Methods*, 2006, **38**, 317.
7 K. L. Kellar and M. A. Iannone, *Exp. Hematol.*, 2002, **30**, 1227.
8 J. P. Nolan and L. A. Sklar, *Trends Biotechnol.*, 2002, **20**, 9.

9 R. Wilson, A. R. Cossins and D. G. Spiller, *Angew. Chem., Int. Ed.*, 2006, **45**, 6104.
10 K. Braeckmans, S. C. De Smedt, M. Leblans, R. Pauwels and J. Demeester, *Nat. Rev. Drug Discovery*, 2002, **1**, 447.
11 R. J. Fulton, R. L. McDade, P. L. Smith, L. J. Kienker and J. R. Kettman, Jr, *Clin. Chem.*, 1997, **43**, 1749.
12 D. A. Vignali, *J. Immunol. Methods*, 2000, **243**, 243.
13 M. J. Benecky, D. R. Post, S. M. Schmitt and M. S. Kochar, *Clin. Chem.*, 1997, **43**, 1764.
14 G. R. Broder, R. T. Ranasinghe, J. K. She, S. Banu, S. W. Birtwell, G. Cavalli, G. S. Galitonov, D. Holmes, H. F. P. Martins, K. F. MacDonald, C. Neylon, N. Zheludev, P. L. Roach and H. Morgan, *Anal. Chem.*, 2008, **80**, 1902.
15 D. C. Pregibon, M. Toner and P. S. Doyle, *Science*, 2007, **315**, 1393.
16 K. C. Nicolaou, K. Ajito, H. Komatsu, B. M. Smith, T. H. Li, M. G. Egan and L. Gomezpaloma, *Angew. Chem., Int. Ed. Engl.*, 1995, **34**, 576.
17 E. J. Moran, S. Sarshar, J. F. Cargill, M. M. Shahbaz, A. Lio, A. M. M. Mjalli and R. W. Armstrong, *J. Am. Chem. Soc.*, 1995, **117**, 10787.
18 W. Mandecki, United States Patent 6,051,377 2000.
19 A. W. Czarnik, *Curr. Opin. Chem. Biol.*, 1997, **1**, 60.
20 D. S. Sebba, D. A. Watson and J. P. Nolan, *ACS Nano*, 2009, **3**, 1477.
21 Y. Zhao, X. Zhao, J. Hu, M. Xu, W. Zhao, L. Sun, Z. C., H. Xu and Z. Gu, *Adv. Mater.*, 2009, **21**, 569.
22 J. Raez, D. R. Blais, Y. Zhang, R. A. Alvarez-Puebla, J. P. Bravo-Vasquez, J. P. Pezacki and H. Fenniri, *Langmuir*, 2007, **23**, 6482.
23 L. Wang, C. Yang and W. Tan, *Nano Lett.*, 2005, **5**, 37.
24 H. Wang, T. Liu, Y. Cao, Z. Huang, J. Wang, X. Li and Y. Zhao, *Anal. Chim. Acta*, 2006, **580**, 18.
25 A. Sukhanova and I. Nabiev, *Crit. Rev. Oncol. Hematol.*, 2008, **68**, 39.
26 X. Gao and S. Nie, *Anal. Chem.*, 2004, **76**, 2406.
27 A. Nanthakumar, R. T. Pon, A. Mazumder, S. Yu and A. Watson, *Bioconjugate Chem.*, 2000, **11**, 282.
28 A. Schnackel, S. Hiller, U. Reibetanz and E. Donath, *Soft Matter*, 2007, **3**, 200.
29 M. Nakamura, M. Shono and K. Ishimura, *Anal. Chem.*, 2007, **79**, 6507.
30 D. Nagao, M. Yokoyama, N. Yamauchi, H. Matsumoto, Y. Kobayashi and M. Konno, *Langmuir*, 2008, **24**, 9804.
31 Q. Liu, J. Liu, J. Guo, X. Yan, D. Wang, L. Chen, F. Yan and L. Chen, *J. Mater. Chem.*, 2009, **19**, 2018.
32 W. Zhang, Y. Han, W. Wang, L. Zhang and J. Chang, *Eur. Polym. J.*, 2009, **45**, 550.
33 D. Nagao, N. Anzai, Y. Kobayashi, S. Gu and M. Konno, *J. Colloid Interface Sci.*, 2006, **298**, 232.
34 S. R. Corrie, G. A. Lawrie and M. Trau, *Langmuir*, 2006, **22**, 2731.
35 M. Nakamura and K. Ishimura, *Langmuir*, 2008, **24**, 5099.
36 M. Nakamura and K. Ishimura, *Langmuir*, 2008, **24**, 12228.
37 Y. Xu, C. Wang, Y. Long, J. Pan and X. Yan, *J. Xiamen Univ. (Nat. Sci.)*, 2008, **47**, 836.
38 H. Lv, Q. Lin, K. Zhang, K. Yu, T. Yao, X. Zhang, J. Zhang and B. Yang, *Langmuir*, 2008, **24**, 13736.
39 O. H. Gonçalves, J. M. Asua, P. H. H. d. Araújo and R. A. F. Machado, *Macromolecules*, 2008, **41**, 6960.
40 Q. Yuan, L. Yang, M. Wang, H. Wang, X. Ge and X. Ge, *Langmuir*, 2009, **25**, 2729.
41 N. Pantelić and C. J. Seliskar, *J. Phys. Chem. C*, 2007, **111**, 18595.
42 V. Martínez Martínez, F. L. Arbeloa, J. B. Prieto, T. A. Lpez and I. L. Arbeloa, *J. Phys. Chem. B*, 2005, **109**, 7443.
43 A. Burns, H. Owb and U. Wiesner, *Chem. Soc. Rev.*, 2006, **35**, 1028.
44 H. Ow, D. R. Larson, M. Srivastava, B. A. Baird, W. W. Webb and U. Wiesner, *Nano Lett.*, 2005, **5**, 113.

This journal is © The Royal Society of Chemistry 2010

J. Mater. Chem., 2010, **20**, 1179–1185 | 1185